ACS OMEGA

Article

Cite This: ACS Omega 2018, 3, 15582−15591

http://pubs.acs.org/journal/acsodf

Homo- and Heteropolymetallic Complexes of the Hybrid, Ambidentate N-Heterocyclic Carbene Ligand IMes-acac

Vincent César,*[,†] Valentina Mallardo,[†] Adela Nano,[‡] Sadie F. DePeter,[†] Stéphanie Bastin,[†] Alix Sournia-Saquet,[†] Aline Maisse-François,[‡] Noël Lugan,[†] and Stéphane Bellemin-Laponnaz*[,‡]

[†]LCC-CNRS, Université de Toulouse, CNRS, Toulouse 31400, France

[‡]IPCMS (Institut de Physique et Chimie des Matériaux de Strasbourg), CNRS-Université de Strasbourg, 23 rue du Loess, BP 43, F-67034 Strasbourg, France

Supporting Information

ABSTRACT: The anionic 5-acetylimidazol-2-ylidene-4-olate **1**$^-$, named as "IMes-acac", is composed of fused diaminocarbene and acetylacetonato units in the same IMes-based imidazolyl ring. The bifunctional compound **1**$^-$ is shown to act as an effective, ditopic bridging ligand for transition metal centers. Several new complexes supported by this ligand were prepared, including the complex [RuCl(*p*-Cym)(κ^2O,O−**1**·H)](BF$_4$) (**2**), which can be regarded as a metallated imidazolium salt, the homobimetallic complex [((COD)Rh)-(RhCl(COD))(μ-1κ^2O,O:2κ^1C−**1**)] (**4**), the heterobimetallic complexes [((*p*-Cym)ClRu)(RhCl(COD))(μ-1κ^2O,O:2κ^1C−**1**)] (**3**), [((*p*-Cym)ClRu)(RhCl(CO)$_2$)(μ-1κ^2O,O:2κ^1C−**1**)] (**5**), [((*p*-Cym)ClRu)(Cu(IPr))(μ-1κ^2O,O:2κ^1C−**1**)] (**9**), the anionic homoleptic Cu(I) complexes [Cu(κ^1C−**1**)$_2$]K ([**10**]K) and [Cu(κ^1C−**1**)$_2$](NEt$_4$) ([**10**](NEt$_4$)), and the heterotrimetallic complex [((*p*-Cym)RuCl)$_2$(Cu)(μ-1κ^2O,O:3κ^1C−**1**)(μ-2κ^2O,O:3κ^1C−**1**)](PF$_6$) (**11**). Preliminary studies on the possible preparation of supramolecular metallopolymers and electrochemical studies on the series of complexes are also reported.

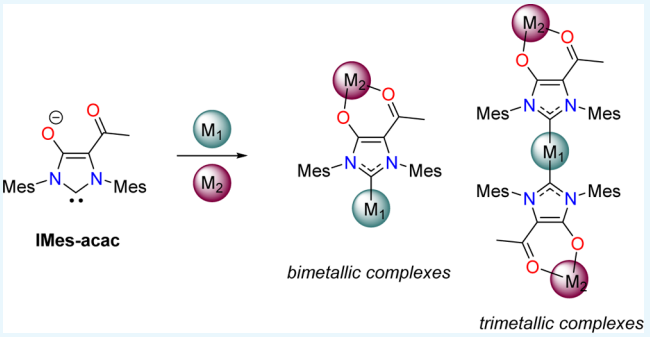

INTRODUCTION

Being strong σ-donor and relatively weak π-acceptor ligands, N-heterocyclic carbenes (NHCs) have been shown to lead to robust organometallic complexes with nearly all transition metals.[1,2] First applications of metal−NHC complexes were found in homogeneous catalysis with the generation of highly efficient and now popular catalytic systems.[3] More recently, NHC-complexes have been applied with great success as highly efficient metallopharmaceuticals,[4] luminescent materials,[5] and other functional materials.[6] The superiority of NHC ligand stems from the thermodynamically strong metal−carbene bond and from the low-kinetic lability of the NHC ligand, avoiding the use of an excess of ligand versus metal center supplemented by the shielding control over the coordination sphere exerted by the wingtip N-substituents.[7] Yet, the most beneficial feature is likely the high modularity of the NHC ligands, whose electronic and steric properties can be easily and independently tuned to match a specific property.[8] The synthetic accesses to the NHC precursors are indeed well established using the countless possibilities of heterocyclic chemistry.[9]

Over the last decade, poly-NHC ligands featuring structurally designed-opposed carbene moieties have been the subject of intense research efforts and have found numerous applications as key-bridging ligands for the construction of discrete polymetallic and metallosupramolecular assemblies, and main-chain organometallic polymers.[10] Alternatively, the design of hybrid and ambidentate NHC ligands, comprising a carbenic moiety and a functional, coordinating group arranged in an opposite fashion into the same scaffold, appeared as a viable and powerful strategy to create new functional discrete and/or polymeric architectures with original properties. Such a bifunctional system would indeed combine the anchoring ligation of the carbenic center with the specific properties brought by the functionalized backbone and would open—inter alia—the opportunity to an electronic communication between both binding sites and even between the two metallic centers. Figure 1 gives an overview of previously reported heteropolymetallic transition-metal complexes supported by hybrid and ambidentate NHC ligands, highlighting the diversity of suitable coordinating backbones.

The association of NHC and phosphorous-based moieties in the same ligand scaffold[11] led to the generation of several heterobimetallic complexes of type **A**,[12] **B**,[13] **C**,[14] and even to the three-dimensional trimetallic system **D**.[15] Metallocene units were also inserted as an integral part of the NHC-skeleton, giving access to bimetallic systems **E**−**H**,[16−19] which were shown to have a dramatic effect on the electronic

Received: September 4, 2018
Accepted: November 6, 2018
Published: November 15, 2018

DOI: 10.1021/acsomega.8b02268
ACS Omega 2018, 3, 15582−15591

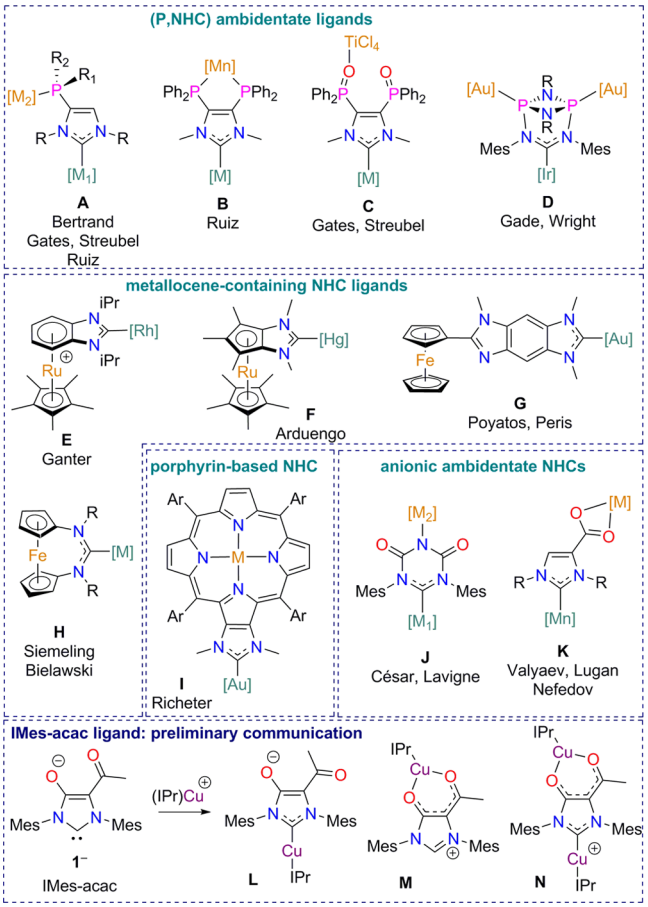

Figure 1. Variety of reported transition metal polymetallic complexes supported by ambidentate and hybrid NHC ligands and preliminary results on the IMes-acetylacetonate (acac) ligand reported in our previous communication.[23] IPr = 1,3-bis(2,6-diisopropylphenyl)-2*H*-imidazole-2-ylidene.

properties of the NHC ligand, thus giving the opportunity to generate redox-active ligand systems. In an analogous approach, the metalation of a porphyrin-fused imidazol-2-ylidene ligand in system **I** had a strong influence on the electronic properties of the NHC.[20] Eventually, our group developed ambidentate and hybrid NHC ligands incorporating an anionic imidato **J** or a carboxylato **K** ligand moiety as a second coordinating unit.[21,22]

In 2015, we introduced the new anionic, hybrid 5-acetylimidazol-2-ylidene-4-olate $\mathbf{1}^-$, named as "IMes-acac", constituted of fused diaminocarbene and acetylacetonato units in the same imidazolyl ring (Figure 1).[23] At that time, we reported the straightforward synthesis of its mesoionic precursor **1**·H, through acetylation of the corresponding 4-hydroxyimidazolium chloride, its generation as a free, stable NHC, and demonstrated its ambidentate character through preliminary coordination studies using the $[(IPr)Cu]^+$ metallic fragment, leading to complexes **L**, **M**, and **N**. We report herein a complete, extended study on the coordination behavior of ligand $\mathbf{1}^-$ toward various metallic centers and coordination geometries (Ru, Rh, Cu, and Au), and on the electronic structure of the resulting complexes, with an emphasis on the possible electronic interaction between both coordinating units within the ligand framework.

RESULTS AND DISCUSSION

Rh(I) and Ru(II) Heterobimetallic Complexes of IMes-acac $\mathbf{1}^-$. The $[RuCl_2(p\text{-Cym})]_2$ and $[RhCl(1,5\text{-COD})]_2$ dimeric precursors were chosen for coordination studies with $\mathbf{1}^-$ because of their ability to form stable complexes with anionic bidentate LX-type and NHC ligands, respectively.[24] In a first approach, no reaction was detected when mesoionic **1**·H was mixed with 0.5 equivalent of $[RuCl_2(p\text{-Cym})]_2$. This behavior is similar to the one previously observed when reacting **1**·H with (IPr)CuCl and confirms the low coordinating and chelating propensity of the acac moiety in mesoionic **1**·H, which is unable to displace a chlorido ligand from the coordination sphere. Actually, subsequent addition of a stoichiometric amount of silver tetrafluoroborate induced the abstraction of one chlorido ligand from the Ru(II) center, allowing the formation of the cationic complex $[RuCl(p\text{-Cym})(\kappa^2O,O\text{-}\mathbf{1}\cdot H)](BF_4)$ (**2**) in an excellent 97% isolated yield (Scheme 1). Complex **2** was fully characterized by

Scheme 1. Synthesis of Rh(I) and Ru(II) Complexes 2−5

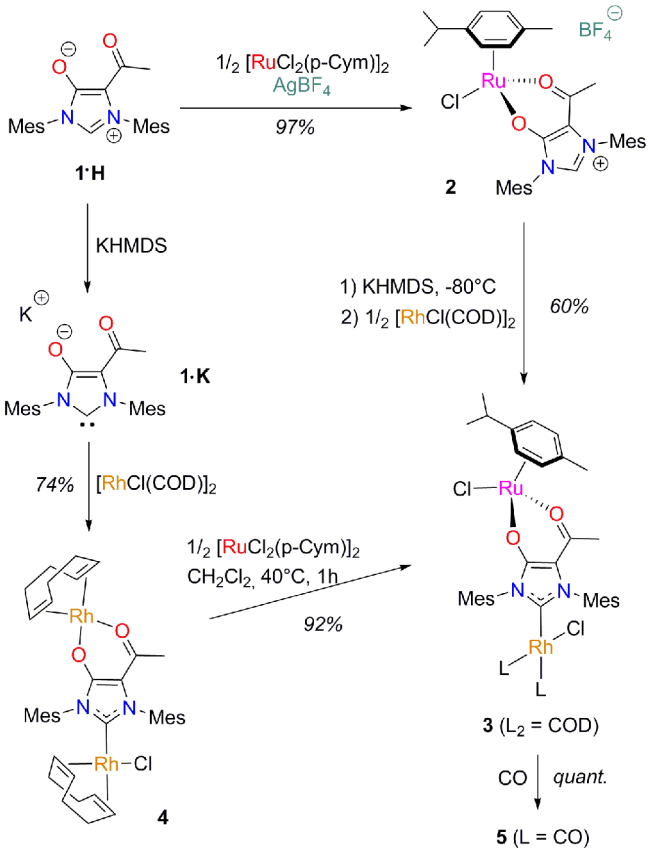

spectroscopic and analytical techniques. Analogously to the previously described complex $[Cu(IPr)(\kappa^2O,O\text{-}\mathbf{1}\cdot H)](BF_4)$, the complexation of the acac moiety of **1**·H in **2** was inferred from the ^{1}H NMR data, which reveal a downfield shift of the imidazolium N_2CH proton from δ 7.23 ppm in mesoionic **1**·H to δ 7.82 ppm in ionic **2**, and an upfield shift of the acetyl protons from δ 2.41 ppm in **1**·H to δ 1.79 ppm in **2**, arising from the placement of the acac-methyl group in the anisotropic cone of the adjacent mesityl substituent upon complexation. The molecular structure of **2** was then confirmed following a single-crystal X-ray diffraction study (Figure 2).[25] Complex **2** displays a distorted pseudo-octahedral geometry around the

DOI: 10.1021/acsomega.8b02268
ACS Omega 2018, 3, 15582−15591

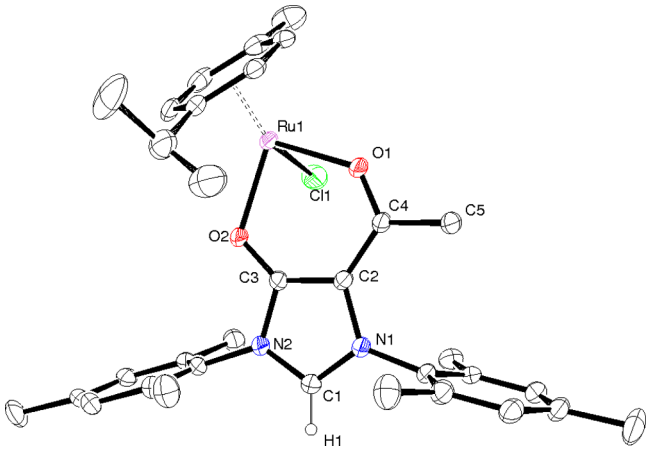

Figure 2. Molecular structure of complex **2** (ellipsoids drawn at 30% probability level). The tetrafluoroborate anion, the cocrystallizing solvent molecule, and hydrogen atoms except H1 were omitted for clarity. Selected bond lengths (Å) and angles (deg): Ru1−O1 2.097(3); Ru1−O2 2.097(3); Ru1−Cl1 2.3881(12); C3−O2 1.253(5); C4−O1 1.246(5); C2−C3 1.399(5); C2−C4 1.424(5); C4−C5 1.497(5); O1−Ru1−O2 88.26(10).

Ru(II) center, in which the *p*-cymene ligand occupies three adjacent coordination sites, and the *acac* backbone of $\mathbf{1}^-$ coordinates the Ru(II) center in a chelating mode. Metrical parameters around the Ru(II) center in **2** are quite analogous to the standard [RuCl(acac)(*p*-Cym)],[26] or to other relevant [RuCl(acylpyrazolonato)(*p*-Cym)] complexes.[27] Complex **2** is chiral-at-metal and crystallizes as a racemate in the centrosymmetric $P2_1/n$ space group.

Although deprotonation of **2** with potassium hexamethyldisilazide (KHMDS) at low temperature and warming up the solution to room temperature led to an intractable mixture of compounds, the direct trapping of the free NHC generated from **2** at low temperature by half an equivalent of $[RhCl(1,5\text{-}COD)]_2$ dimer gave the stable heterobimetallic complex $[RuCl(p\text{-}Cym)][RhCl(COD)](\mu\text{-}1\kappa^2\text{-}O,O\text{:}2\kappa^1C\text{−}\mathbf{1})$ (**3**) in 60% yield after purification. On contrary to complex **2**, which has to be handled under strict inert conditions, complex **3** is an air- and water-stable compound and could be easily isolated by column chromatography. Its formulation was confirmed by ^{1}H and ^{13}C NMR spectroscopy. The three components of the complex, that is $[RuCl(p\text{-}Cym)]^+$, ligand $\mathbf{1}^-$, and RhCl(COD), appear in the ^{1}H NMR spectrum as distinct sets of signals for each of them and the respective integrations of the respective signals are 1/1/1. In addition, the appearance in the ^{13}C NMR spectrum of a doublet at δ 194.1 ppm (J_{Rh-C} = 52 Hz) is the signature of the formation of a RhCl(NHC)(COD) complex.

At that point, we were wondering whether complex **3** could be synthesized through the reverse sequence of complexation that is first, complexation of the NHC part and then complexation of the anionic acac "upper" part. Contrarily to our previous observation with other anionic backbone-functionalized NHCs,[28] the reaction between the generated free NHC **1**·K with 0.5 equivalent of $[RhCl(1,5\text{-}COD)]_2$ dimer did not lead to the expected anionic $[RhCl(COD)(\kappa^1C\text{−}\mathbf{1})]^-$ complex, but to the hitherto uncommon bimetallic complex $[(COD)Rh][RhCl(COD)](\mu\text{-}1\kappa^2O,O\text{:}2\kappa^1C\text{−}\mathbf{1})$ (**4**), in which $\mathbf{1}^-$ behaves as a bridging ambidentate ligand. Complex **4** was subsequently obtained in 74% yield by altering the stoichiometry of $[RhCl(1,5\text{-}COD)]_2$ to one equivalent. Complex **4** is an air- and water-stable compound and was purified by column chromatography. The formation of the Rh−C_{NHC} bond was evidenced by a doublet at δ 192.5 ppm (J_{Rh-C} = 52 Hz) appearing in the ^{13}C NMR spectrum of **4**, and the formation of the di-rhodium complex was assessed by the observation of two different coordinated COD ligands in both ^{1}H and ^{13}C NMR spectra. This is the first time we observed such a direct double complexation on $\mathbf{1}^-$ from a single metallic precursor. This reactivity pattern can be easily explained in terms of the electronic nature of the metallic fragment coordinated to the carbenic center. Indeed, we had previously observed that $\mathbf{1}^-$ is able to displace the chlorido ligand in (IPr)CuCl to generate the zwitterionic complex $[Cu(\kappa^1C\text{−}\mathbf{1})(IPr)]$ (**L**) (see Figure 1), in which the carbenic part is coordinated to the cationic $[Cu(IPr)]^+$ fragment. Here, ligand $\mathbf{1}^-$ is thought to break the $[RhCl(COD)]_2$ dimer to generate the anionic complex $[RhCl(\kappa^1C\text{−}\mathbf{1})(COD)]^-$, in which the carbenic part is coordinated to the neutral [RhCl(COD)] fragment. Because of this overall charge difference, the pending *acac* moiety in $[RhCl(\kappa^1C\text{−}\mathbf{1})(COD)]^-$ has now a restored nucleophilicity and can displace the chlorido ligand from the second [RhCl(COD)] fragment released during the dimer-breaking process. Attempts to efficiently demetalate the *acac* moiety in **4** were unsuccessful. Indeed, although, according to ^{1}H NMR of the crude mixture, treatment of **4** with an excess of HCl led to the complete formation of $[RhCl(COD)]_2$ and the protonated complex $[RhCl(\kappa^1C\text{−}\mathbf{1}^{OH})(COD)]$, we were unable to isolate the latter complex neither by column chromatography (complex **4** was reformed under these conditions) nor by selective precipitation of $[RhCl(COD)]_2$ by carrying out the reaction in methanol (see the Supporting Information for details). Yet, to our delight, the $[Rh(COD)]^+$ fragment could be cleanly exchanged for the $[RuCl(p\text{-}Cym)]^+$ fragment by mixing complex **4** with 0.5 equivalent of $[RuCl_2(p\text{-}Cym)]_2$ to afford heterobimetallic complex **3** in 92% yield, along with the $[RhCl(COD)]_2$ dimer as the byproduct isolated in 95% yield. The latter reactivity is the testimony of the lability of the *acac* moiety versus the carbenic part in ligand $\mathbf{1}^-$.

Complex **3** was converted into its dicarbonyl derivative $[(p\text{-}Cym)ClRu][RhCl(CO)_2](\mu\text{-}1\kappa^2O,O\text{:}2\kappa^1C\text{−}\mathbf{1})$ (**5**) by bubbling CO gas into a solution of the complex in CH_2Cl_2 at room temperature. The carbonylation reaction is selective of the rhodium part, leaving the ruthenium fragment unaffected. Measuring the average IR-stretching frequency of the carbonyl ligands in **5** allowed assessing of the electron-donor ability of the metallated NHC ligand "$\mathbf{1}^{RuCl(p\text{-}Cym)}$". The average frequency value ν_{av}^{CO} = 2039 cm^{-1} gives, after linear regression, a Tolman electronic parameter (TEP) of 2051.5 cm^{-1}, which corresponds to an electronic donation for $\mathbf{1}^{RuCl(p\text{-}Cym)}$ quite similar to the one of the standard IMes ligand (TEP = 2050.8 cm^{-1}).[7b]

Group 11 and Ru(II) Heterometallic Complexes of IMes-acac $\mathbf{1}^-$. Previously, we reported that the anionic carbene **1**·K easily displaces the chlorido ligand from (IPr)CuCl to afford the zwitterionic, heteroleptic complex $[Cu(\kappa^1C\text{−}\mathbf{1})(IPr)]$ (**6** or **L**) in 92% yield (Scheme 2).[23] The same reactivity pattern was observed against (IPr)AuCl leading to complex $[Au(\kappa^1C\text{−}\mathbf{1})(IPr)]$ (**7**) isolated in 72% yield. Complex **7** was fully characterized by spectroscopic and analytical means. In the ^{13}C NMR spectrum, the chemical shifts of the carbenic centers of IPr and $\mathbf{1}^-$ ligands at δ = 182.5 and 176.9 ppm, respectively, are similar to the ones previously

DOI: 10.1021/acsomega.8b02268
ACS Omega 2018, 3, 15582−15591

Scheme 2. Synthesis of Zwitterionic Complexes 6−7 and of Heterobimetallic Complex 9

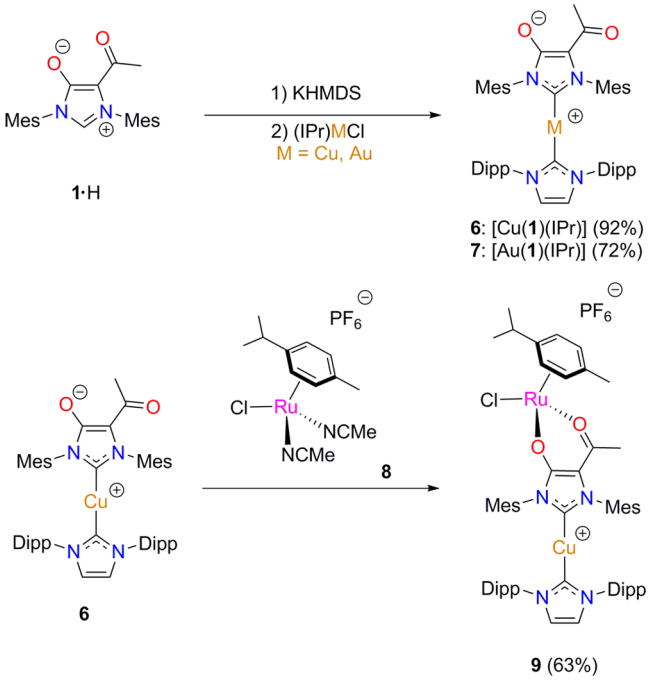

Scheme 3. Synthesis of Anionic, Heteroleptic Complexes [10]⁻ and of the Heterotrimetallic Complex 11

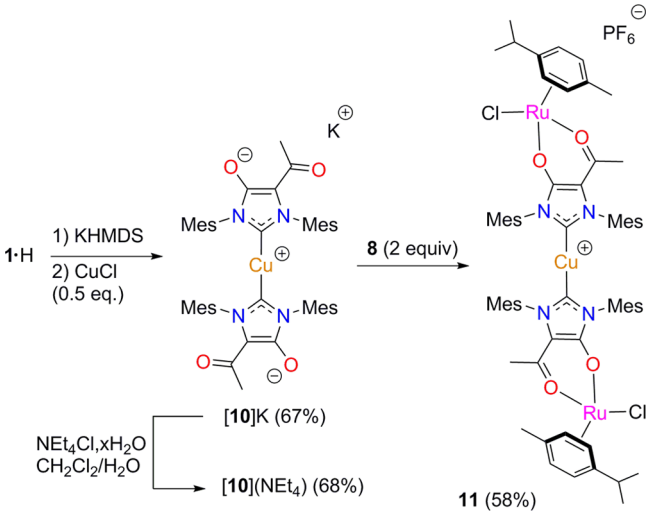

reported for related, cationic gold−bis(NHC) complexes.[29] The cationic, heterodinuclear complex {[(*p*-Cym)RuCl][Cu(IPr)]}(μ-1κ^2*O*,*O*:2κ^1*C*−**1**)}(PF_6) (**9**) was obtained in 63% yield by treating the zwitterionic complex **6** with the cationic Ru(II) precursor [RuCl(CH_3CN)$_2$(*p*-Cym)](PF_6) (**8**). The carbenic carbon atoms of the IPr and **1**$^-$ NHC ligands in **8** are now observed at δ 179.0 ppm and δ 177.3 ppm, respectively. Again, the complexation of the ruthenium fragment onto the *acac* backbone was accompanied by the shielding of the acetyl protons from δ = 2.22 ppm in **6** to δ = 1.29 ppm in **9**, and the loss of symmetry from C_v in **6** (one mirror plane) to C_1 in **9** because of the presence of the chiral ruthenium center. Consequences in the NMR spectra are mainly concentrated on the signals of the mesityl groups, which are all split.

Altering the reaction stoichiometry between **1**·K and CuCl to a 2:1 ratio led to the novel, anionic, and homoleptic complex [Cu(κ^1*C*−**1**)$_2$]K ([**10**]·K) (Scheme 3). The reaction appeared to be complete in 2 h at 40 °C as judged by NMR of the crude product. The desired complex was isolated in 67% yield as a beige powder after evaporation of all volatiles and simple washings with Et_2O and water to remove organic and KCl byproducts, respectively. Because of the insolubility of [**10**]K in common organic solvents, a salt metathesis was carried out by adding an excess of $NEt_4Cl{\cdot}xH_2O$ in the biphasic mixture CH_2Cl_2/H_2O to afford the complex [**10**](NEt$_4$), isolated in 68% yield. [**10**](NEt$_4$) was found readily soluble in CH_2Cl_2, $CHCl_3$, acetone, and tetrahydrofuran (THF) but insoluble in Et_2O and hydrocarbons. The formulation of **10**$^-$ as the bis-NHC copper(I) complex [Cu(κ^1*C*−**1**)$_2$]$^-$ was inferred from the ^{13}C NMR spectrum, the resonance of the two carbene carbon nuclei being observed at δ = 174.0 ppm, a value comparable to the ^{13}C carbenic resonance at δ = 178.8 ppm in [Cu(IMes)$_2$]$^+$,[30] and by mass spectrometry in the negative electrospray ionization mode, exhibiting a single peak at m/z = 785 a.u. corresponding to the anion [Cu(κ^1*C*−**1**)$_2$]$^-$. Eventually, because of the symmetry of the molecule, only one set of signals was observed in the NMR profiles for the two ligands **1**$^-$. Addition of two equivalents of complex [RuCl(CH_3CN)$_2$(*p*-Cym)](PF_6) (**8**) allowed for the capping of the complex **10**$^-$ by coordination of the *acac* moieties to two ruthenium centers. The resulting heterotrimetallic complex {[RuCl(*p*-Cym)]$_2$[Cu](μ-1κ^2*O*,*O*:3κ^1*C*−**1**)(μ-2κ^2*O*,*O*:3κ^1*C*−**1**)}(PF_6) (**11**) was isolated in 58% yield as an air-and moisture-stable red powder. In the ^{1}H and ^{13}C NMR spectra of complex **11**, all but a few resonances are split into two signals of equal intensity evidencing the presence of two diastereoisomers for complex **11**, namely the racemic mixture (S_{Ru},S_{Ru})-**11**/(R_{Ru},R_{Ru})-**11**, and the *meso* compound (S_{Ru},R_{Ru})-**11**, in a 1/1 ratio.

Because **10**$^-$ has shown its ability to act as a ditopic ligand with ruthenium to generate heterotrimetallic complex **11**, we next investigated the potential of **10**$^-$ to generate supramolecular metallopolymers by simply mixing the ligand with a suitable metal ion in solution. Such self-assembly processes may be easily monitored by UV−vis titration. However, employing Ni(BF_4)$_2$ or Cu(BF_4)$_2$ as metal sources, titration experiments led to the in situ formation of discrete trimetallic species {[M]$_2$[Cu](μ-1κ^2*O*,*O*:3κ^1*C*−**1**)(μ-2κ^2*O*,*O*:3κ^1*C*−**1**)} (M = Cu or Ni fragments) instead of metallopolymeric entities (see Figures S13 and S14).[31] These data also confirmed the low ability of the *acac* moiety in **10**$^-$ to generate homoleptic species, probably due to electrostatic repulsion.

Electrochemical Studies. The correlation between the substitution pattern of ligand **1**$^-$ and the redox properties of the different redox-active parts of its complexes **2**−**7** and **9**−**11** was evaluated by cyclic voltammetry (CV) and square-wave voltammetry (SQW). The CV analysis of precursor **1**·H in CH_2Cl_2 shows an irreversible oxidation wave at $E_{p,a}$ = + 1.39 V versus saturated calomel electrode (SCE) (Figure 3) that could be assigned to the one-electron oxidation of the anionic *acac* moiety to generate the radical cation [**1**·H]$^{\bullet+}$, which decomposed rapidly.[32] No other redox process could be detected within the full potential range (Figure S2 in the Supporting Information). Interestingly, the oxidation process became reversible at high scan rates, typically above 50 V s^{-1} (Figure S3). The uncoordinated *acac* backbone is also present in the zwitterionic complexes **6** and **7** and in complex

DOI: 10.1021/acsomega.8b02268
ACS Omega 2018, 3, 15582−15591

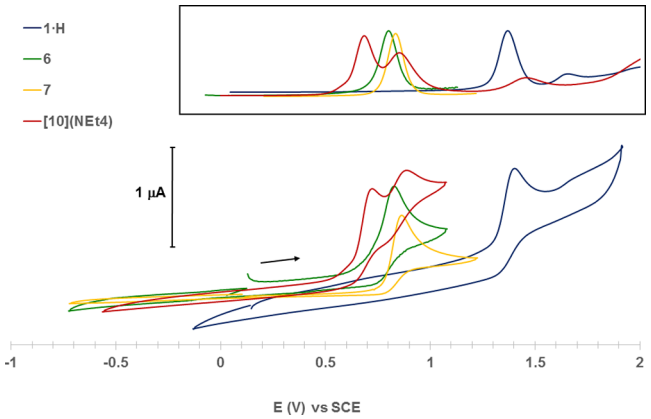

Figure 3. CV plots and relevant SQW sections (inset) of **1**·H (in blue) and complexes **6** (in green), **7** (in orange), and [**10**](NEt$_4$) (in red) (1 mM in CH_2Cl_2 with 0.1 M Bu_4NPF_6 as the supporting electrolyte, 200 mV s^{-1} scan rate, spectra calibrated against Fc/Fc$^+$ using as the internal standard with $E_{1/2}$ = 0.46 V vs. SCE).

Table 1. Cyclic Voltammetric Data for Complexes 2, 3, 4, 5, 9, and 11 in the Anodic Range[a]

complex	E [V vs SCE] [Rh^I/Rh^{II}]	E [V vs SCE] unattributed	E [V vs SCE] [Ru^{II}/Ru^{III}]
2			1.60 (rev.)[b]
3	0.86 (rev.)		1.49 (ir.)
4	0.87 (ir.)	1.14 (ir.), 1.34 (rev.)	
5	1.32 (ir.)		1.51 (ir.)
9			1.41 (ir.)
11			1.44 (ir.)

[a]CV recorded in CH_2Cl_2 (10^{-3} M) with 0.1 M [nBu$_4$N][PF$_6$] at a Pt microdisk working electrode. Sweep rate: 200 mV s^{-1}. Potentials are given relative to SCE. Anodic peak potential $E_{p,a}$ is quoted for irreversible (ir.) processes. The potentials for the reversible (rev.) couples are defined as the mean of the anodic and cathodic peak potentials $E_{1/2} = (E_{p,a} + E_{p,c})/2$. Spectra were calibrated by adding ferrocene at the end of the experiments (Fc/Fc$^+$: 0.46 V vs SCE in CH_2Cl_2).[34] Assignments of the oxidation wave given when possible. [b]A small irreversible oxidation wave was also observed at $E_{p,a}$ = 1.39 V due to free **1**·H.

[**10**](NEt$_4$). Similarly to precursor **1**·H, we observed only one irreversible oxidation wave at $E_{p,a}$ = 0.82 V versus SCE in the cyclic voltammogram of complex **6**, which was assigned to one-electron oxidation of the *acac* backbone. However, the significantly lower oxidation potential, from $E_{p,a}$ = 1.39 V in **1**·H to $E_{p,a}$ = 0.82 V versus SCE in **6**, indicated a strong influence of the substitution of the N_2C carbon atom on the electronic density within the structure of ligand **1**$^-$. This was further confirmed by the CV data of the isostructural, gold(I) complex **7** because the same irreversible oxidation process occurred at $E_{p,a}$ = 0.86 V versus SCE. Although the close values of the oxidation potentials for **6** and **7** spoke for oxidation localized on the same part of the complexes, namely the *acac* ligand, the difference of 40 mV between them confirmed the electronic connection of the carbene and *acac* parts within the ligand heterocycle. Eventually, two irreversible oxidation waves at $E_{p,a1}$ = 0.70 V versus SCE and $E_{p,a2}$ = 0.87 V versus SCE were clearly identified in the CV of the homoleptic anionic complex [**10**]$^-$, and could be reasonably assigned to the successive oxidation of the two distal, *acac* backbones of ligands **1**$^-$ in [**10**]$^-$. In particular, the lower oxidation potential of the first wave at $E_{p,a1}$ = 0.70 V versus SCE compared to the one of **6** ($E_{p,a}$ = 0.82 V vs. SCE) indicates that the *acac* moiety and thus the Cu(I) center were more electron-rich in [**10**]$^-$ than in **7**. This constituted an indirect proof that ligand **1**$^-$ is more electron-donating than the standard IPr. As the redox processes were irreversible, no other conclusion could be drawn concerning the second oxidation wave at $E_{p,a2}$ = 0.87 V versus SCE.

The cyclic voltammogram of complex **2** shows a reversible 1e$^-$ oxidation wave at $E_{1/2}$ = 1.60 V versus SCE that can be assigned to the redox couple Ru^{II}/Ru^{III} (Table 1). Three oxidation processes were detected for bis-rhodium complex **4**. The first irreversible oxidation wave at $E_{p,a}$ = 0.87 V versus SCE corresponds to the couple Rh^I/Rh^{II} where the rhodium center is coordinated to the carbene center of **1**$^-$ as its potential compares well with the redox potential of metal-centered oxidation of analogous monometallic RhCl(NHC)(COD) complexes.[33] This process became reversible when the CV measurements were stopped at 1 V versus SCE as the upper limit and with a sweep rate higher than 10 V s^{-1}. Interestingly, the redox process Rh^I/Rh^{II} was found to be fully reversible in the hetero bimetallic complex **3**, ($E_{1/2}$ = 0.86 V vs SCE), which is very close to the one previously reported for complex RhCl(IMes)(COD) at $E_{1/2}$ = 0.83 V under the same conditions.[33c] This definitely confirms that the metallo-NHC ligand **1**$^{\mathbf{RuCl(}p\text{-}\mathbf{Cym)}}$ exerts a similar overall electronic donation to the metal as IMes. The second irreversible wave at $E_{p,a}$ = 1.49 V versus SCE in the CV of **3** most probably corresponds to the Ru^{II}/Ru^{III} redox couple, and the shift of the potential to lower values compared to **2**, from 1.60 V in **2** to 1.49 V in **3**, indicates here again that the nature of the group on the N_2C carbon atom has an impact on the redox properties of the *acac* part. The same trend was observed in the cyclic voltammograms of Cu/Ru bimetallic complex **9** and Ru/Cu/Ru trimetallic complex **11**, in which the Ru^{II} oxidation processes were found irreversible at $E_{p,a}$ = 1.41 and 1.44 V versus SCE, respectively. Moreover, the absence of splitting and of broadening of the oxidation band for **11** ruled out any possible electronic communication between the two Ru centers in **11**. This result was quite expected taking into account the long distance between the two distal ruthenium centers.

Summary. We have conducted a complete exploration of the coordination chemistry of the hybrid ambidentate IMes-acac ligand **1**$^-$, obtained by fusing a diaminocarbene and an *acac* unit into the same carbenic heterocycle. The ability of ligand **1**$^-$ to act as an effective ditopic bridging ligand for transition metal centers has been shown with the synthesis and the full characterization of a series of homo- and hetero-polymetallic complexes incorporating Ru(II), Rh(I), Cu(I), and Au(I) centers. Noteworthy, while the carbene center strongly binds the metal ions in all cases, the coordinating strength of the pending *acac* moiety depends on the nature and the charge of the group ligated onto the carbenic part, and ranges from quite low in the mesoionic precursor **1**·H to strong when the carbene center coordinates a neutral Rh(I) fragment. In the preliminary studies aiming at the formation of supramolecular metallopolymers, discrete trimetallic complexes were formed instead, reflecting the poor tendency of two ligands **1**$^-$ to coordinate the same metal center in a homoleptic mode through their respective *acac* functionality. The electrochemical measurements on the complexes indicate an electronic interaction between the two parts of IMes-acac, but the extent of the electronic communication between the

DOI: 10.1021/acsomega.8b02268
ACS Omega 2018, 3, 15582−15591

two distal metallic centers through ligand 1^- remains quite low. We are therefore considering further developments aiming at improving both the coordinating strength of the functional backbone and the electronic communication within the carbenic scaffold by increasing the denticity of the ligand unit on the backbone, by changing the nature of the coordinating atoms, or by modifying the size and structure of the carbenic heterocycle.

EXPERIMENTAL SECTION

Materials and Methods. All manipulations were performed under an inert atmosphere of dry nitrogen by using standard vacuum line and Schlenk tube techniques. The glassware was dried at 120 °C in an oven for at least 3 h. Toluene, CH_2Cl_2, pentane, Et_2O, and THF were dried using an SPS system from Innovative Technology and water content was quantified by Karl Fischer titration. Dimethylformamide was deoxygenated by bubbling N_2 for 15 min and was stored over activated 4Å molecular sieves.

NMR spectra were recorded on Bruker AV300 or AV400 spectrometers. Chemical shifts are reported in ppm (δ) compared to tetramethylsilane (^1H and ^{13}C) using the residual peak of deuterated solvent as the internal standard.[35] Infrared spectra were obtained on a PerkinElmer Spectrum 100 FT-IR spectrometer. Microanalyses were performed by the Micro Analytical Services of the LCC and MS spectra by the mass spectrometry service of the "Institut de Chimie de Toulouse".

1,3-dimesityl-5-acetylimidazolium-4-olate **1**·H,[23] [RhCl(COD)]$_2$,[36] [RuCl$_2$(*p*-cymene)]$_2$,[37] [RuCl(CH$_3$CN)$_2$(*p*-Cym)](PF$_6$) (**8**),[38] (IPr)CuCl,[39] and (IPr)AuCl[40] were synthesized according to literature procedures. All other reagents were commercially available and used as received.

Complex [RuCl(*p*-Cym)(κ^2*O*,*O*−1·H)](BF$_4$) (2). To a solution of [RuCl$_2$(*p*-Cym)]$_2$ (99 mg, 0.162 mmol, 0.5 equiv) in CH$_3$CN (5 mL), AgBF$_4$ (63 mg, 0.323 mmol, 1.0 equiv) was added at room temperature. After 5 min, **1**·H (117 mg, 0.323 mmol) was added as a solid and the reaction mixture was stirred for additional 40 min. The mixture was concentrated under vacuum and the residue was taken up in CH_2Cl_2 (5 mL) and filtered using a filtering cannula and the solvent was evaporated under vacuum. The residue was washed twice with Et_2O (2 × 5 mL) and dried under vacuum to afford an orange powder (226 mg, 97%). ^1H NMR (400 MHz, $CDCl_3$): δ 7.82 (s, 1H, N$_2$C*H*), 7.08 (s, 1H, C*H*$_{Mes}$), 7.06 (s, 1H, C*H*$_{Mes}$), 6.97 (s, 2H, C*H*$_{Mes}$), 5.67−5.65 (m, 1H, C*H*$_{p\text{-}Cym}$), 5.62−5.61 (m, 1H, C*H*$_{p\text{-}Cym}$), 5.49−5.47 (m, 2H, C*H*$_{p\text{-}Cym}$), 2.79−2.72 (m, 1H, C*H*$_{iPr}$), 2.36 (s, 3H, C*H*$_3$), 2.35 (s, 3H, C*H*$_3$), 2.34 (s, 3H, C*H*$_3$), 2.28 (s, 3H, C*H*$_3$), 2.13 (s, 3H, C*H*$_3$), 2.06 (s, 3H, C*H*$_3$), 1.99 (s, 3H, C*H*$_3$), 1.79 (s, 3H, C*H*$_3$CO), 1.22 (pseudo t, J = 7.1 Hz, 6H, C*H*$_{3iPr}$); $^{13}C\{^1H\}$ NMR (100.5 MHz, $CDCl_3$): δ 187.0 (*C*═O), 158.3 (*C*$_{Im}$−O$^-$), 142.1, 141.0, 135.8, 135.6, 134.9 (*C*$_{Mes}$), 133.8 (N$_2$*C*H), 130.5, 130.0, 129.7, 129.5 (*C*H$_{Mes}$), 112.8 (*C*$_{Im\text{-}5}$), 99.5 (*C*$_{p\text{-}Cym}$), 96.9 (*C*$_{p\text{-}Cym}$), 82.8 (*C*H$_{p\text{-}Cym}$), 81.7 (*C*H$_{p\text{-}Cym}$), 80.0 (*C*H$_{p\text{-}Cym}$), 79.8 (*C*H$_{p\text{-}Cym}$), 31.0 (*C*H$_{iPr}$), 25.6 (*C*H$_3$CO), 22.2 (*C*H$_{3iPr}$), 21.9 (*C*H$_{3iPr}$), 21.4, 18.4, 17.9, 17.7, 17.5, 17.2 (*C*H$_{3Mes}$ + *C*H$_{3p\text{-}Cym}$); IR (ATR) $\tilde{\nu}$: 3604, 2966, 2923, 1638, 1560, 1473, 1226, 1032, 854, 819, 737 cm^{-1}; MS (ESI) m/z (%): 633 (11) [M − BF$_4$]$^+$, 363 (100) [M − BF$_4$ − (RuCl(*p*-Cym)) + H]$^+$; elemental Anal. Calcd (%) for C$_{33}$H$_{40}$BClF$_4$N$_2$O$_2$Ru (MW = 720.02): C, 55.05; H, 5.60; N, 3.89. Found: C, 55.29; H, 5.42; N, 3.70.

Complex [((*p*-Cym)ClRu)(RhCl(COD))(μ-1κ^2*O*,*O*:2κ^1*C*−1)] (3). *Starting from Complex 4.* Complex **4** (72.2 mg, 88.1 μmol) and [RuCl$_2$(*p*-cymene)]$_2$ (29.7 mg, 48.5 μmol, 0.55 equiv) were dissolved in CH_2Cl_2 (4 mL) and the solution was stirred 2 h at 40 °C. The mixture was loaded directly onto a silica gel column. The first bright yellow fraction eluting with pure CH_2Cl_2 obtained after evaporation and drying [RhCl(COD)$_2$]$_2$ (20.0 mg, 95%), and the second orange fraction was then eluted using CH_2Cl_2/MeOH: 95/5 as the solvent mixture, which is obtained after evaporation and drying the title product as an orange powder (71.5 mg, 92%).

Starting from Complex 2. A solution of KHMDS (0.5 M in toluene, 380 μL, 0.189 mmol, 1.05 equiv) was added dropwise to a solution of complex **2** (130 mg, 0.180 mmol, 1.0 equiv) in THF (10 mL) at −80 °C, resulting in slight darkening of the orange solution. After 20 min, [RhCl(COD)]$_2$ (44.5 mg, 0.09 mmol, 0.50 equiv) was added as a solid to the reaction mixture and the solution was stirred in the cooling bath for 6 h. After removing the latter, all volatiles were removed in vacuo and the dark red residue was purified by flash chromatography (SiO$_2$, CH_2Cl_2/MeOH: 99/1) to give an orange powder (95 mg, 60%).

^1H NMR (400 MHz, $CDCl_3$): δ 7.05 (s, 1H, C*H*$_{Mes}$), 7.03 (s, 1H, C*H*$_{Mes}$), 6.96 (s, 1H, C*H*$_{Mes}$), 6.87 (s, 1H, C*H*$_{Mes}$), 5.40−5.29 (m, 2H, C*H*$_{Cym}$), 5.17 (d, J = 5.5 Hz, 1H, C*H*$_{Cym}$), 5.13 (d, J = 5.6 Hz, 1H, C*H*$_{Cym}$), 4.49 (br, 2H, C*H*$_{COD}$), 3.36 (br, 1H, C*H*$_{COD}$), 3.09 (br, 1H, C*H*$_{COD}$), 2.68 (sept, J = 6.9 Hz, 1H, C*H*$_{iPr}$), 2.57 (s, 3H, C*H*$_3$), 2.44 (s, 3H, C*H*$_3$), 2.38 (s, 3H, C*H*$_3$), 2.35 (s, 3H, C*H*$_3$), 2.16 (s, 3H, C*H*$_3$), 2.11 (s, 3H, C*H*$_3$), 1.87 (s, 3H, C*H*$_3$), 1.78−1.61 (m, 4H, C*H*$_{2COD}$), 1.57 (s, 3H, C*H*$_3$CO), 1.54−1.44 (m, 4H, C*H*$_{2COD}$), 1.16 (pseudo t, J = 6.1 Hz, 6H, C*H*$_{3iPr}$); $^{13}C\{^1H\}$ NMR (100.5 MHz, $CDCl_3$): δ 194.1 (d, J_{Rh-C} = 52.3 Hz, N$_2$*C*), 178.1 (*C*═O), 161.7 (*C*$_{Im\text{-}4}$−O), 139.0, 138.4, 138.0, 137.8, 136.2, 135.9, 132.6 (*C*$_{Mes}$), 129.9, 129.1, 128.6, 128.2 (*C*H$_{Mes}$), 116.0 (*C*$_{Im\text{-}5}$), 99.6 (*C*$_{Cym}$), 97.6 (d, J_{Rh-C} = 7.1 Hz, *C*H$_{COD}$), 97.1 (d, J_{Rh-C} = 7.1 Hz, *C*H$_{COD}$), 96.4 (*C*$_{Cym}$), 82.3, 82.0, 79.3, 79.1(*C*H$_{Cym}$), 68.3 (d, J_{Rh-C} = 14.4 Hz, *C*H$_{COD}$), 67.5 (d, J_{Rh-C} = 14.4 Hz, *C*H$_{COD}$), 33.0, 32.3 (*C*H$_{2COD}$), 31.0 (*C*H$_{iPr}$), 28.5, 28.0 (*C*H$_{2COD}$), 24.3 (*C*H$_3$CO), 22.2, 22.0 (*C*H$_{3iPr}$), 21.3, 21.2, 20.5, 20.3 (*C*H$_{3o\text{-}Mes}$), 19.4 (*C*H$_{3Cym}$), 18.4, 17.8 (*C*H$_{3p\text{-}Mes}$); MS (ESI) m/z (%): 843 (5) [M − Cl]$^+$, 573 (100) [H(acac-IMes)Rh(COD)]$^+$, 565 (17) [Ru$_2$Cl$_3$(*p*-Cym)$_2$ − Me]$^+$; elemental Anal. Calcd (%) for C$_{41}$H$_{51}$Cl$_2$N$_2$O$_2$RhRu (MW = 878.75): C, 56.04; H, 5.85; N, 3.19. Found: C, 55.72; H, 5.50; N, 3.00.

Complex [((COD)Rh)(RhCl(COD))(μ-1κ^2*O*,*O*:2κ^1*C*−1)] (4). A solution of KHMDS (0.5 M in toluene, 0.75 mL, 0.375 mmol, 1.1 equiv) was added dropwise to a solution of **1**·H (124 mg, 0.341 mmol) in THF (10 mL) at room temperature. After 15 min, [RhCl(COD)]$_2$ (168 mg, 0.341 mmol, 1.0 equiv) was added as a solid to the solution which became immediately dark red. After 3 h, all volatiles were removed under vacuum and the crude residue was purified by flash chromatography (SiO$_2$, CH_2Cl_2/MeOH: 95/5) to yield a yellow powder (206 mg, 74%). ^1H NMR (400 MHz, $CDCl_3$): δ 7.03 (s, 1H, C*H*$_{Mes}$), 6.99 (s, 1H, C*H*$_{Mes}$), 6.96 (s, 1H, C*H*$_{Mes}$), 6.92 (s, 1H, C*H*$_{Mes}$), 4.46 (br s, 2 H, C*H*$_{COD}$), 4.02−3.98 (m, 2H, C*H*$_{COD}$), 3.92 (br s, 2H, C*H*$_{COD}$), 3.30 (br s, 1H, C*H*$_{COD}$), 3.24 (br s, 1H, C*H*$_{COD}$), 2.47−2.32 (m, 6H, C*H*$_{2COD}$), 2.40 (s, 3H, C*H*$_{3ortho}$), 2.34 (s, 3H, C*H*$_{3ortho}$), 2.34 (s, 3H, C*H*$_{3ortho}$), 2.31 (s, 3H, C*H*$_{3ortho}$), 2.06 (s, 3H, C*H*$_{3para}$), 2.01 (s, 3H, C*H*$_{3para}$), 1.77−1.62 (m, 8H, C*H*$_{2COD}$), 1.52 (s,

DOI: 10.1021/acsomega.8b02268
ACS Omega 2018, 3, 15582−15591

3H, CH_3CO), 1.50−1.47 (m, 2H, CH_{2COD}); $^{13}C\{^1H\}$ NMR (100.5 MHz, $CDCl_3$): δ 192.5 (d, J_{Rh-C} = 52.4 Hz, N_2C), 178.4 (C═O), 161.8 (C_{Im-4}−O^-), 139.2, 138.8, 138.4, 138.3, 135.9, 135.6, 135.2, 132.5 (C_{Mes}), 130.1, 129.6, 128.2, 127.8 (CH_{Mes}), 115.4 (C_{Im-5}), 97.5 (d, J_{Rh-C} = 7.2 Hz, CH_{COD}), 77.3 (d, J_{Rh-C} = 14.3 Hz, CH_{COD}), 77.0 (d, J_{Rh-C} = 14.2 Hz, CH_{COD}), 76.0 (d, J_{Rh-C} = 14.5 Hz, CH_{COD}), 75.4 (d, J_{Rh-C} = 14.5 Hz, CH_{COD}), 68.0 (d, J_{Rh-C} = 14.5 Hz, CH_{COD}), 67.7 (d, J_{Rh-C} = 14.3 Hz, CH_{COD}), 32.7, 30.3, 30.2, 30.0, 28.3, 28.2 (CH_{2COD}), 24.4 (CH_3CO), 21.3, 21.2, 20.2, 20.1 (CH_{3ortho}), 18.8, 18.5 (CH_{3para}); IR (ATR): ν = 2995, 2915, 2873, 2826, 1611, 1606, 1479, 1442, 1401, 1380, 1309, 1287, 1209, 1131, 965, 831, 756 cm^{-1}; MS (ESI) m/z (%): 783 (3) $[M - Cl]^+$, 573 (100) $[H(acac\text{-}IMes)Rh(COD)]^+$, 363 (5) $[(acac\text{-}IMes)\text{-}H]^+$; elemental Anal. Calcd (%) for $C_{39}H_{49}ClN_2O_2Rh_2$ (MW = 819.09): C, 57.19; H, 6.03; N, 3.42. Found: C, 56.75; H, 5.67; N, 3.15.

Complex [((*p*-Cym)ClRu)(RhCl(CO)$_2$)(μ-1κ^2*O*,*O*:2κ^1*C*−1)] (5). At room temperature, CO gas was bubbled into a solution of complex **3** (101 mg, 0.115 mmol) in CH_2Cl_2 (6 mL) for 10 min during which the orange color slightly faded. After 40 min, all volatiles were removed under vacuum and the residue was washed with pentane (3 × 3 mL) to yield after drying an orange powder (83 mg, 87%). ^1H NMR (400 MHz, $CDCl_3$): δ 6.96 (s, 2H, CH_{Mes}), 6.95 (s, 1H, CH_{Mes}), 6.92 (s, 1H, CH_{Mes}), 5.45−5.42 (m, 2H, CH_{Cym}), 5.22 (d, J = 5.7 Hz, 1H, CH_{Cym}), 5.18 (d, J = 5.7 Hz, 1H, CH_{Cym}), 2.70 (sept, J = 6.9 Hz, 1H, CH_{iPr}), 2.35 (s, 3H, CH_3), 2.34 (s, 6H, CH_3), 2.30 (s, 3H, CH_3), 2.14 (s, 3H, CH_3), 2.13 (s, 3H, CH_3), 2.03 (s, 3H, CH_3), 1.59 (s, 3H, CH_3CO), 1.18 (pseudo-t, J = 6.7 Hz, 6H, CH_{3iPr}); $^{13}C\{^1H\}$ NMR (100.5 MHz, $CDCl_3$): δ 185.0 (d, J_{Rh-C} = 53.9 Hz, Rh−CO), 183.6 (d, J_{Rh-C} = 45.0 Hz, N_2C_{carb}), 182.6 (d, J_{Rh-C} = 74.7 Hz, Rh−CO), 180.9 (C═O), 161.7 (C_{Im-4}−O), 139.8, 139.0, 136.5, 136.4, 136.2, 135.1131.4 (C_{Mes}), 129.6, 129.6, 129.2, 128.8 (CH_{Mes}), 115.2 (C_{Im-5}), 99.6 (C_{Cym}), 96.6 (C_{Cym}), 82.5, 81.9, 79.3, 79.0 (CH_{Cym}), 31.1 (CH_{iPr}), 24.5 (CH_3CO), 22.2, 22.0 (CH_{3iPr}), 21.4, 19.3, 19.2, 19.1, 18.2, 17.9 (CH_{3Mes} + CH_{3Cym}); IR (CH_2Cl_2) ν: 2080, 1998 cm^{-1}; IR (ATR) ν: 2960 (w), 2922 (w), 2869 (w), 2069 (vs, C═O), 1986 (vs, C═O), 1621 (vs, C═O), 1485 (s), 1460 (m), 1409 (m), 1379 (m) 1318 (m), 1294 (m), 1217 (m), 1135 (m), 1033 (w), 971 (m), 837 (m) cm^{-1}; MS (ESI) m/z (%): 793 (19) $[M - Cl]^+$, 763 (12) $[M - Cl - CO]^+$, 565 (100) $[Ru_2Cl_3(p\text{-}Cym)_2 - Me]^+$; elemental Anal. Calcd (%) for $C_{35}H_{39}Cl_2N_2O_4RhRu$ (MW = 826.58): C, 50.86; H, 4.76; N, 3.39. Found: C, 50.46; H, 4.36; N, 3.18.

Complex [Au(IPr)(κ^1*C*−1)] (7). A solution of KHMDS (0.5 M in toluene, 0.93 mL, 0.465 mmol, 1.15 equiv) was added dropwise to a solution of **1**·H (160 mg, 0.403 mmol, 1.0 equiv) in THF (20 mL) at room temperature. After 15 min, AuCl(IPr) (250 mg, 0.403 mmol, 1.0 equiv) was added and the mixture was stirred for 3 h. After evaporation of volatiles, the crude product was purified by flash chromatography (SiO_2, pure CH_2Cl_2 then CH_2Cl_2/MeOH: 95/5) to yield a beige powder. Further crystallization in CH_2Cl_2/Et_2O furnished the pure product as an off-white powder (275 mg, 72%). ^1H NMR (300 MHz, $CDCl_3$): δ 7.53 (t, J = 7.8 Hz, 2H, CH_{Dipp-p}), 7.16 (d, J = 7.8 Hz, 4H, CH_{Dipp-m}), 7.04 (s, 2H, CH_{Im}), 6.67 (s, 2H, CH_{Mes}), 6.57 (s, 2H, CH_{Mes}), 2.33−2.24 (m, 14H, CH_{3Mes} + CH_{iPr}), 1.77 (s, 6H, CH_{3ortho}), 1.70 (s, 6H, CH_{3ortho}), 1.64 (s, 3H, CH_3CO), 1.08 (d, J = 6.8 Hz, 12H, CH_{3iPr}), 0.91 (d, J = 6.9 Hz, 12H, CH_{3iPr}); $^{13}C\{^1H\}$ NMR (75.5 MHz, $CDCl_3$): δ 189.4 (C═O), 182.5 (N_2C_{IPr}), 176.9 ($N_2C_{IMes\text{-}acac}$), 161.0 (C_{Im}−O^-), 145.1, 137.6, 136.9, 136.1, 135.8, 134.5, 133.8, 132.7 (C_{Ar}), 130.6 (CH_{Dipp-p}), 129.2 (CH_{Mes}), 128.7 (CH_{Mes}), 124.1 (CH_{Dipp-m}), 123.4 (CH_{Im}), 108.9 (C_{Im-5}), 28.7 (CH_{iPr}), 26.4 (CH_3−C═O), 23.95 (CH_{3iPr}), 23.9 (CH_{3iPr}), 21.5 (CH_{3para}), 21.4 (CH_{3para}), 18.0 (CH_{3ortho}), 17.5 (CH_{3ortho}); MS (ESI) m/z (%): 969 (17) $[M + Na]^+$, 947 (100) $[M + H]^+$; elemental Anal. Calcd (%) for $C_{50}H_{61}AuN_4O_2$ (MW = 947.03): C, 63.41; H, 6.49; N, 5.92. Found: C, 63.12; H, 6.33; N, 5.85.

Complex [((*p*-Cym)ClRu)(Cu(IPr))(μ-1κ^2*O*,*O*:2κ^1*C*−1)] (9). A solution of $[RuCl(p\text{-}Cym)(CH_3CN)_2](PF_6)$ (114 mg, 0.228 mmol, 1.1 equiv) in CH_2Cl_2 (5 mL) was added to solid **6** (169 mg, 0.208 mmol, 1.0 equiv) at room temperature. The TLC controller indicated that the reaction was finished after 15 min. The solution was then evaporated and the crude product was purified by flash chromatography (SiO_2, CH_2Cl_2/MeOH: 100/0 to 95/5) to yield the pure product as an orange powder (161 mg, 63%). ^1H NMR (400 MHz, $CDCl_3$): δ 7.53 (t, J = 7.8 Hz, 2H, CH_{Dipp-p}), 7.19−7.13 (m, 4H, CH_{Dipp-m}), 7.07 (s, 2H, CH_{Im}), 6.77 (s, 1H, CH_{Mes}), 6.70 (s, 1H, CH_{Mes}), 6.67 (s, 2H, CH_{Mes}), 5.39−5.36 (m, 2H, CH_{Cym}), 5.21 (d, J = 6.1 Hz, 2H, CH_{Cym}), 2.59−2.46 (m, 1H, CH_{iPr}), 2.37 (s, 3H, $CH_{3p\text{-}Mes}$), 2.33 (s, 3H, $CH_{3p\text{-}Mes}$), 2.31−2.23 (m, 4H, CH_{iPr}), 2.00 (s, 3H, CH_{3Cym}), 1.76 (s, 3H, $CH_{3o\text{-}Mes}$), 1.71 (s, 3H, $CH_{3o\text{-}Mes}$), 1.60 (s, 3H, $CH_{3o\text{-}Mes}$), 1.57 (s, 3H, $CH_{3o\text{-}Mes}$), 1.29 (s, 3H, CH_3CO), 1.08−1.03 (m, 18H, CH_{3iPr}), 0.88 (d, J = 6.9 Hz, 6H, CH_{3iPr}), 0.70 (d, J = 6.9 Hz, 6H, CH_{3iPr}); $^{13}C\{^1H\}$ NMR (100.5 MHz, $CDCl_3$): δ 182.7 (C═O), 179.0 (N_2C_{IPr}), 177.3 ($N_2C_{IMes\text{-}acac}$), 160.8 (C_{Im}−O^-), 145.0 (C_{Dipp}), 139.5, 138.5, 136.0, 135.7, 135.5, 135.4 (C_{Mes}), 134.2 (C_{Dipp}), 130.7 (CH_{Dipp}), 130.1, 129.7, 129.6, 129.3 (CH_{Mes}), 124.3, 124.2 (CH_{Dipp}), 124.0(CH_{Im}), 113.4 (C_{Im-5}), 99.3, 96.2 (C_{Cym}), 82.4, 81.5, 79.7, 79.6 (CH_{Cym}), 30.9 (CH_{iPr}), 28.7, 28.6 (CH_{iPr}), 24.6 (CH_3CO), 24.6, 24.2, 23.7, 23.5 (CH_{3iPr}), 22.0, 21.7 (CH_{3iPr}), 21.4, 21.3 ($CH_{3p\text{-}Mes}$), 18.4, 17.7, 17.5, 17.4 ($CH_{3o\text{-}Mes}$), 17.2 (CH_{3Cym}); MS (ESI): m/z (%): 1085 (39) $[M - PF_6]^+$, 813 (11) $[M - PF_6 - RuCl(p\text{-}Cym) + H]^+$, 524 (100) $[M - PF_6 - Cl]^{2+}$; HRMS (ESI) m/z: calcd for $C_6H_{75}ClCuN_4O_2Ru$, 1083.3929; found, 1083.3953, ε_r = 2.2 ppm.

Complex [Cu(κ^1*C*−1)$_2$]K [10]K. A solution of KHMDS (0.5 M in toluene, 2.2 mL, 1.1 mmol, 1.1 equiv) was added dropwise to a solution of **1**·H (362.5 mg, 1.0 mmol) in THF (15 mL) at room temperature. After 15 min, CuCl (49.5 mg, 0.5 mmol, 0.5 equiv) was added and the mixture was stirred at 40 °C for 2 h. After evaporation of volatiles, the work-up was carried out in air. Et_2O (15 mL) was added and the mixture was filtered through a fritted funnel. The crude residue was washed with additional Et_2O (2 × 10 mL) and water (3 × 5 mL). The solid was then dissolved in acetone and dried over Na_2SO_4. Filtration and evaporation led to a beige powder (279 mg, 67%). ^1H NMR (400 MHz, DMSO-d_6): δ 6.87 (s, 4H, CH_{Mes}), 6.72 (s, 4H, CH_{Mes}), 2.32 (s, 6H, CH_{3para}), 2.30 (s, 6H, CH_{3para}), 2.01 (s, 6H, CH_3CO), 1.61 (s, 12H, CH_{3ortho}), 1.54 (s, 12H, CH_{3ortho}); $^{13}C\{^1H\}$ NMR (100.5 MHz, DMSO-d_6): δ 178.4 (C═O), 174.0 (N_2C_{carb}), 160.0 (C_{Im-4}−O), 139.0, 136.6, 135.4, 135.3, 134.0, 133.8 (C_{Mes}), 128.0, 127.5 (CH_{Mes}), 107.4 (C_{Im-5}), 25.4 (CH_3CO), 20.7 (CH_{3para}), 17.3, 16.8 (CH_{3ortho}); MS (ESI, negative mode): m/z (%): 785 (100) $[M - K]^-$; HRMS (ESI) m/z: calcd for $C_{46}H_{50}N_4O_4{}^{63}Cu$, 785.3128; found, 785.3107, ε_r = 2.7 ppm.

Complex [Cu(κ^1*C*−1)$_2$](NEt$_4$) [10](NEt$_4$). A solution of KHMDS (477 mg, 2.39 mmol, 1.05 equiv) in THF (15 mL)

DOI: 10.1021/acsomega.8b02268
ACS Omega 2018, 3, 15582−15591

was added dropwise to a solution of **1**·H (825 mg, 2.28 mmol) in THF (20 mL) at room temperature. After 20 min, CuCl (112 mg, 1.13 mmol, 0.5 equiv) was added and the mixture was stirred at 40 °C for 2 h. The brown mixture was then evaporated to dryness and the solid residue was taken up in CH_2Cl_2 (20 mL). Water (20 mL) and a large excess of $NEt_4Cl\cdot xH_2O$ were added and the two phase mixture was vigorously stirred. The organic layer was then extracted and washed with water (2 × 20 mL) and dried over Na_2SO_4. After filtration through a cotton plug, the solution was evaporated and the crude residue was purified by flash chromatography (neutral Al_2O_3, Brockmann type III, CH_2Cl_2 then CH_2Cl_2/MeOH 95/5) to yield a light brown powder (463 mg, 45%). ^{1}H NMR (400 MHz, $CDCl_3$): δ 6.79 (s, 4H, CH_{Mes}), 6.68 (s, 4H, CH_{Mes}), 3.01 (br, 8H, $N-CH_2-CH_3$), 2.30 (s, 6H, CH_{3para}), 2.28 (s, 6H, CH_{3para}), 1.69 (s, 12H, CH_{3ortho}), 1.61 (s, 12H, CH_{3ortho}), 1.21 (s, 6H, CH_3CO), 1.04 (br, 16H, $N-CH_2-CH_3$); ^{13}C{^{1}H} NMR (100.5 MHz, $CDCl_3$): δ 181.1 (C=O), 174.7 (N_2C_{carb}), 161.3 ($C_{Im\text{-}4}$–O), 139.2, 137.2, 136.1, 134.7, 134.0 (C_{Mes}), 128.4, 127.9 (CH_{Mes}), 108.9 ($C_{Im\text{-}5}$), 52.2 ($N-CH_2-CH_3$), 29.3 (CH_3CO), 21.3 (CH_{3para}), 21.2 (CH_{3para}), 17.9, 17.4 (CH_{3ortho}), 7.5 ($N-CH_2-CH_3$); MS (ESI, negative mode): m/z (%): 785 (100) $[M - NEt_4]^-$.

Complex [((*p*-Cym)RuCl)$_2$(Cu)(μ-1κ^2*O*,*O*:3κ^1*C*−1)(μ-2κ^2*O*,*O*:3κ^1*C*−1)](PF$_6$) (11). Complex [**10**]K (150 mg, 0.18 mmol, 1.0 equiv) and [RuCl(*p*-Cym)$(CH_3CN)_2$](PF_6) (181.3 mg, 0.36 mmol, 2.0 equiv) were combined in CH_2Cl_2 (5 mL) at room temperature. The solution was stirred for 15 min then loaded directly onto a silica gel column and eluted with CH_2Cl_2/MeOH: 95/5. One fraction was collected and evaporated using a rotary evaporator, then dissolved in the minimum of CH_2Cl_2. The product precipitated with sonication. The liquid was decanted off and drying of the yellow solid gave the final product (155 mg, 58%). ^{1}H NMR (400 MHz, $CDCl_3$) δ 6.89 (s, 1H, CH_{Mes}), 6.87 (s, 1H, CH_{Mes}), 6.86 (s, 1H, CH_{Mes}), 6.84 (s, 2H, CH_{Mes}), 6.82 (s, 1H, CH_{Mes}), 6.79 (s, 1H, CH_{Mes}), 6.76 (s, 1H, CH_{Mes}), 5.44–5.40 (dd, 4H, $CH_{p\text{-}Cym}$), 5.23–5.20 (dd, 4H, $CH_{p\text{-}Cym}$), 2.69–2.59 (m, 2H, CH_{iPr}), 2.38 (s, 6H, CH_{3para}), 2.35 (s, 6H, CH_{3para}), 2.06 (s, 6H, $CH_{3p\text{-}Cym}$), 1.73 (s, 3H, CH_{3ortho}), 1.71 (s, 3H, CH_{3ortho}), 1.69 (s, 3H, CH_{3ortho}), 1.67 (s, 3H, CH_{3ortho}), 1.62 (s, 3H, CH_{3ortho}), 1.57 (s, 3H, CH_{3ortho}), 1.51 (s, 6H, CH_3CO), 1.49 (s, 3H, CH_{3ortho}), 1.47 (s, 3H, CH_{3ortho}), 1.15–1.12 (dd, 12H, CH_{3iPr}); ^{13}C NMR (101 MHz, $CDCl_3$): δ 182.4 (C=O), 182.2 (C=O), 179.3 (N_2C), 160.7 ($C_{Im\text{-}4}$–O), 139.9 (C_{Mes}), 139.8 (C_{Mes}), 139.2 (C_{Mes}), 136.1 (C_{Mes}), 135.7 (C_{Mes}), 135.1 (C_{Mes}), 134.8 (C_{Mes}), 131.0 (C_{Mes}), 129.4 (CH_{Mes}), 129.3 (CH_{Mes}), 129.0 (CH_{Mes}), 128.8 (CH_{Mes}), 113.3 ($C_{Im\text{-}5}$), 113.2 ($C_{Im\text{-}5}$), 99.5 ($C_{p\text{-}Cym}$), 99.4 ($C_{p\text{-}Cym}$), 96.5 ($C_{p\text{-}Cym}$), 96.4 ($C_{p\text{-}Cym}$), 82.4 ($CH_{p\text{-}Cym}$), 82.3 ($CH_{p\text{-}Cym}$), 81.8 ($CH_{p\text{-}Cym}$), 81.7 ($CH_{p\text{-}Cym}$), 79.4 ($CH_{p\text{-}Cym}$), 79.3 ($CH_{p\text{-}Cym}$), 79.2 ($CH_{p\text{-}Cym}$), 30.9 (CH_{iPr}), 24.7 (CH_3CO), 22.1 (CH_{3iPr}), 21.9 (CH_{3iPr}), 21.4 (CH_{3para}), 21.3 (CH_{3para}), 18.3 (CH_{3ortho}), 18.2 (CH_{3ortho}), 17.7 ($CH_{3p\text{-}Cym}$), 17.6 (CH_{3ortho}), 17.5 (CH_{3ortho}), 17.4 (CH_{3ortho}), 17.3 (CH_{3ortho}), 16.9 (CH_{3ortho}), 16.8 (CH_{3ortho}); MS (ESI) m/z (%): 1329 (1) $[M - PF_6]^+$, 1059 (11) $[M - PF_6 - RuCl(p\text{-Cym}) + H]^+$, 787 (19) $[M - PF_6 - 2\,RuCl(p\text{-Cym}) + 2H]^+$, 646 (9) $[M - PF_6 - Cl]^{2+}$, 511 (100) $[M - PF_6 - RuCl_2(p\text{-Cym}) + H]^{2+}$; HRMS (ESI) m/z: calcd for $C_{66}H_{78}Cl_2CuN_4O_4Ru_2$, 1327.8000; found, 1327.2784, ε_r = 1.2 ppm.

Electrochemical Studies. The electrochemical properties of these compounds were determined by CV and SQW.

CV and SQW experiments were carried out with an Autolab PGSTAT100 potentiostat (Metrohm). Electrochemical measurements were performed with a three-electrode system consisting of a platinum working electrode (0.5 mm diameter microdisk), a platinum counter electrode, and a SCE as the reference electrode (separated from the solution by a bridge compartment). Experiments were carried out under argon in degassed, distilled CH_2Cl_2, using 0.1 M ^{n}Bu$_4$NPF$_6$ as the supporting electrolyte and using a typical concentration of compound of 10^{-3} M. Spectra were referenced versus the SCE, and were calibrated against Fc^+/Fc redox couple by adding ferrocene at the end of the experiments [$E_{1/2}(Fc^+/Fc)$ = + 0.46 V vs SCE].

Square-wave voltammograms were obtained using an amplitude of 20 mV, a frequency of 20 Hz, and a step potential of 5 mV.

X-ray Diffraction Study of Complex [RuCl(*p*-Cym)-(κ^2*O*,*O*−1)](BF$_4$) (2). Single crystals of **2** were grown by slow diffusion of Et_2O into a solution of **2** in CH_2Cl_2 at room temperature. Data were collected at 100 K on a Bruker D8/APEX II/Incoatec IμS Microsource diffractometer. All calculations were performed on a PC compatible computer using the WinGX system.[41] The structures were solved using the SIR92 program,[42] which revealed in each instance the position of most of the nonhydrogen atoms. The complex was found to crystallize with half a molecule of dichloromethane per unit cell. Atomic scattering factors were taken from the international tables for X-ray crystallography. All non-hydrogen atoms were resolved by the full matrix least-squares method using the SHELXL program,[43] and were refined anisotropically. Anomalous dispersion terms for Ru and Cl were included in Fc. From an initial, idealized positioning (C–H in the range 0.93–0.98 Å, and U_{iso}(H) in the range 1.2–1.5 times U_{equiv} of the attached carbon atom), the H atoms were refined as "riding" atoms. CCDC 1865121 contains the supplementary crystallographic data for the structure of **2**. These data can be obtained free of charge from the Cambridge Crystallographic Data Centre via www.ccdc.cam.ac.uk/data_request/cif.

■ ASSOCIATED CONTENT

Supporting Information

The Supporting Information is available free of charge on the ACS Publications website at DOI: 10.1021/acsomega.8b02268.

Detailed description of reaction of complex **4** with HCl, electrochemical studies, titration experiments of [**10**] with different metal salts, and NMR spectra (PDF)

Crystallographic data for the structure of **2** (CIF)

■ AUTHOR INFORMATION

Corresponding Authors

*E-mail: vincent.cesar@lcc-toulouse.fr (V.C.).
*E-mail: bellemin@unistra.fr (S.B.-L.).

ORCID

Vincent César: 0000-0002-6203-6434
Noël Lugan: 0000-0002-3744-5252
Stéphane Bellemin-Laponnaz: 0000-0001-9462-5703

Notes

The authors declare no competing financial interest.

DOI: 10.1021/acsomega.8b02268
ACS Omega 2018, 3, 15582–15591

■ ACKNOWLEDGMENTS

Financial support by the CNRS is gratefully acknowledged. V.M. thanks the University of Bari Aldo Moro for doctoral internship grant. S.F.D. thanks the NSF for "Research Experiences for Undergraduates" (REU) grant. This work has been supported in part by the Strasbourg IDEX program and we thank the NIE Labex for support (ANR-11-LABX-0058_NIE).

■ REFERENCES

(1) For selected recent monographs on NHC chemistry, see: (a) Díéz-González, S. *N-Heterocyclic Carbenes: From Laboratory Curiosities to Efficient Synthetic Tools*, 2nd ed.; RSC: Cambridge, U.K., 2017. (b) Nolan, S. P. *N-Heterocyclic Carbenes: Effective Tools for Organometallic Synthesis*; Wiley-VCH: Weinheim, Germany, 2014. (c) Cazin, C. S. J. N-Heterocyclic Carbenes in Transition Metal Catalysis and Organocatalysis. *Catalysis by Metal Complexes*; Springer: Berlin, Germany, 2011; Vol. *32*.

(2) (a) Hopkinson, M. N.; Richter, C.; Schedler, M.; Glorius, F. An overview of N-heterocyclic carbenes. *Nature* **2014**, *510*, 485−496. (b) Bourissou, D.; Guerret, O.; Gabbaï, F. P.; Bertrand, G. Stable Carbenes. *Chem. Rev.* **2000**, *100*, 39−92.

(3) (a) Bellemin-Laponnaz, S.; Dagorne, S. Group 1 and 2 and Early Transition Metal Complexes Bearing N-Heterocyclic Carbene Ligands: Coordination Chemistry, Reactivity, and Applications. *Chem. Rev.* **2014**, *114*, 8747−8774. (b) Riener, K.; Haslinger, S.; Raba, A.; Högerl, M. P.; Cokoja, M.; Herrmann, W. A.; Kühn, F. E. Chemistry of Iron N-Heterocyclic Carbene Complexes: Syntheses, Structures, Reactivities, and Catalytic Applications. *Chem. Rev.* **2014**, *114*, 5215−5272. (c) Díez-González, S.; Marion, N.; Nolan, S. P. N-Heterocyclic Carbenes in Late Transition Metal Catalysis. *Chem. Rev.* **2009**, *109*, 3612−3676.

(4) (a) Liu, W.; Gust, R. Update on metal N-heterocyclic carbene complexes as potential anti-tumor metallodrugs. *Coord. Chem. Rev.* **2016**, *329*, 191−213. (b) Liu, W.; Gust, R. Metal N-heterocyclic carbene complexes as potential antitumor metallodrugs. *Chem. Soc. Rev.* **2013**, *42*, 755−773. (c) Hindi, K. M.; Panzner, M. J.; Tessier, C. A.; Cannon, C. L.; Youngs, W. J. The Medicinal Applications of Imidazolium Carbene−Metal Complexes. *Chem. Rev.* **2009**, *109*, 3859−3884.

(5) (a) Strassner, T. Phosphorescent Platinum(II) Complexes with C^C* Cyclometalated NHC Ligands. *Acc. Chem. Res.* **2016**, *49*, 2680−2689. (b) Visbal, R.; Gimeno, M. C. N-heterocyclic carbene metal complexes: photoluminescence and applications. *Chem. Soc. Rev.* **2014**, *43*, 3551−3574.

(6) (a) Zhukhovitskiy, A. V.; MacLeod, M. J.; Johnson, J. A. Carbene Ligands in Surface Chemistry: From Stabilization of Discrete Elemental Allotropes to Modification of Nanoscale and Bulk Substrates. *Chem. Rev.* **2015**, *115*, 11503−11532. (b) Mercs, L.; Albrecht, M. Beyond catalysis: N-heterocyclic carbene complexes as components for medicinal, luminescent, and functional materials applications. *Chem. Soc. Rev.* **2010**, *39*, 1903−1912.

(7) (a) Gómez-Suárez, A.; Nelson, D. J.; Nolan, S. P. Quantifying and understanding the steric properties of N-heterocyclic carbenes. *Chem. Commun.* **2017**, *53*, 2650−2660. (b) Nelson, D. J.; Nolan, S. P. Quantifying and understanding the electronic properties of N-heterocyclic carbenes. *Chem. Soc. Rev.* **2013**, *42*, 6723−6753.

(8) Munz, D. Pushing Electrons-Which Carbene Ligand for Which Application? *Organometallics* **2018**, *37*, 275−289.

(9) Benhamou, L.; Chardon, E.; Lavigne, G.; Bellemin-Laponnaz, S.; César, V. Synthetic Routes to N-Heterocyclic Carbene Precursors. *Chem. Rev.* **2011**, *111*, 2705−2733.

(10) For selected reviews, see: (a) Sinha, N.; Hahn, F. E. Metallosupramolecular Architectures Obtained from Poly-N-heterocyclic Carbene Ligands. *Acc. Chem. Res.* **2017**, *50*, 2167−2184. (b) Peris, E. Polyaromatic N-heterocyclic carbene ligands and π-stacking. Catalytic consequences. *Chem. Commun.* **2016**, *52*, 5777−5787. (c) Waters, J. B.; Goicoechea, J. M. Coordination chemistry of ditopic carbanionic N-heterocyclic carbenes. *Coord. Chem. Rev.* **2015**, *293*−*294*, 80−94. (d) Mata, J. A.; Hahn, F. E.; Peris, E. Heterometallic complexes, tandem catalysis and catalytic cooperativity. *Chem. Sci.* **2014**, *5*, 1723−1732. (e) Neilson, B. M.; Tennyson, A. G.; Bielawski, C. W. Advances in bis(N-heterocyclic carbene) chemistry: new classes of structurally dynamic materials. *J. Phys. Org. Chem.* **2012**, *25*, 531−543.

(11) For a review, see: Gaillard, S.; Renaud, J.-L. When phosphorus and NHC (N-heterocyclic carbene) meet each other. *Dalton Trans.* **2013**, *42*, 7255−7270.

(12) (a) Han, Z.; Bates, J. I.; Strehl, D.; Patrick, B. O.; Gates, D. P. Homo- and Heteropolynuclear Complexes Containing Bidentate Bridging 4-Phosphino-N-Heterocyclic Carbene Ligands. *Inorg. Chem.* **2016**, *55*, 5071−5078. (b) Ruiz, J.; Mesa, A. F.; Sol, D. 1,3-Dimethyl-4-(diphenylphosphino)imidazolium Triflate: A Functionalized Ionic Liquid with Ambivalent Coordination Capability. *Organometallics* **2015**, *34*, 5129−5135. (c) Mendoza-Espinosa, D.; Donnadieu, B.; Bertrand, G. Facile Preparation of Homo- and Hetero-Dimetallic Complexes with a 4-Phosphino-Substituted NHC Ligand. Toward the Design of Multifunctional Catalysts. *Chem.—Asian J.* **2011**, *6*, 1099−1103.

(13) Ruiz, J.; Mesa, A. F. A 4,5-Diphosphino-Substituted Imidazolium Salt: A Building Block for the Modular Synthesis of Mixed Diphosphine-NHC Heterometallic Complexes. *Chem.—Eur. J.* **2012**, *18*, 4485−4488.

(14) Majhi, P. K.; Serin, S. C.; Schnakenburg, G.; Gates, D. P.; Streubel, R. Mono- and Hetero-Dinuclear Complexes of Janus-Head NHC Ligands Possessing Backbone Phosphinoyl Groups: the Case of Soft and Hard Metal Centers. *Eur. J. Inorg. Chem.* **2014**, 4975−4983.

(15) Roth, T.; Vasilenko, V.; Benson, C. G. M.; Wadepohl, H.; Wright, D. S.; Gade, L. H. Extending N-heterocyclic carbene ligands into the third dimension: a new type of hybrid phosphazane/NHC system. *Chem. Sci.* **2015**, *6*, 2506−2510.

(16) (a) Hildebrandt, B.; Raub, S.; Frank, W.; Ganter, C. Expanding the Chemistry of Cationic N-Heterocyclic Carbenes: Alternative Synthesis, Reactivity, and Coordination Chemistry. *Chem.—Eur. J.* **2012**, *18*, 6670−6678. (b) Hildebrandt, B.; Frank, W.; Ganter, C. A Cationic N-Heterocyclic Carbene with an Organometallic Backbone: Synthesis and Reactivity. *Organometallics* **2011**, *30*, 3483−3486.

(17) Arduengo, A. J.; Tapu, D.; Marshall, W. J. The Generation of a Metallocene-Fused Imidazol-2-ylidene and Its Mercury Complex. *Angew. Chem., Int. Ed.* **2005**, *44*, 7240−7244.

(18) Ibáñez, S.; Poyatos, M.; Dawe, L. N.; Gusev, D.; Peris, E. Ferrocenyl-Imidazolylidene Ligand for Redox-Switchable Gold-Based Catalysis. A Detailed Study on the Redox-Switching Abilities of the Ligand. *Organometallics* **2016**, *35*, 2747−2758.

(19) (a) Rittinghaus, S.; Färber, C.; Bruhn, C.; Siemeling, U. Unsymmetrical N-heterocyclic carbenes with a 1,1′-ferrocenediyl backbone. *Dalton Trans.* **2014**, *43*, 3508−3520. (b) Siemeling, U.; Färber, C.; Bruhn, C. A stable crystalline N-heterocyclic carbene with a 1,1′-ferrocenediyl backbone. *Chem. Commun.* **2009**, 98−100. (c) Khramov, D. M.; Rosen, E. L.; Lynch, V. M.; Bielawski, C. W. Diaminocarbene[3]ferrocenophanes and Their Transition-Metal Complexes. *Angew. Chem., Int. Ed.* **2008**, *47*, 2267−2270.

(20) (a) Longevial, J.-F.; Langlois, A.; Buisson, A.; Devillers, C. H.; Clément, S.; van der Lee, A.; Harvey, P. D.; Richeter, S. Synthesis, Characterization, and Electronic Properties of Porphyrins Conjugated with N-Heterocyclic Carbene (NHC)-Gold(I) Complexes. *Organometallics* **2016**, *35*, 663−672. (b) Lefebvre, J.-F.; Lo, M.; Gisselbrecht, J.-P.; Coulembier, O.; Clément, S.; Richeter, S. Porphyrins Fused to N-Heterocyclic Carbenes (NHCs): Modulation of the Electronic and Catalytic Properties of NHCs by the Central Metal of the Porphyrin. *Chem.—Eur. J.* **2013**, *19*, 15652−15660.

(21) Vujkovic, N.; César, V.; Lugan, N.; Lavigne, G. An Ambidentate Janus-Type Ligand System Based on Fused Carbene and Imidato Functionalities. *Chem.—Eur. J.* **2011**, *17*, 13151−13155.

(22) Valyaev, D. A.; Uvarova, M. A.; Grineva, A. A.; César, V.; Nefedov, S. N.; Lugan, N. Post-coordination backbone functionalization of an imidazol-2-ylidene and its application to synthesize

DOI: 10.1021/acsomega.8b02268
ACS Omega 2018, 3, 15582−15591

heteropolymetallic complexes incorporating the ambidentate IMesCO$_2^-$ ligand. *Dalton Trans.* **2016**, *45*, 11953−11957.
(23) César, V.; Mallardo, V.; Nano, A.; Dahm, G.; Lugan, N.; Lavigne, G.; Bellemin-Laponnaz, S. IMes-acac: hybrid combination of diaminocarbene and acetylacetonato sub-units into a new anionic ambidentate NHC ligand. *Chem. Commun.* **2015**, *51*, 5271−5274.
(24) [RuCl(O^O)(p-Cym)] were repeatedly reported in literature. See for recent examples: (a) Pettinari, R.; Marchetti, F.; Petrini, A.; Pettinari, C.; Lupidi, G.; Smoleński, P.; Scopelliti, R.; Riedel, T.; Dyson, P. J. From Sunscreen to Anticancer Agent: Ruthenium(II) Arene Avobenzone Complexes Display Potent Anticancer Activity. *Organometallics* **2016**, *35*, 3734−3742. (b) Singh, N.; Jang, S.; Jo, J.-H.; Kim, D. H.; Park, D. W.; Kim, I.; Kim, H.; Kang, S. C.; Chi, K.-W. Coordination-Driven Self-Assembly and Anticancer Potency Studies of Ruthenium−Cobalt-Based Heterometallic Rectangles. *Chem.—Eur. J.* **2016**, *22*, 16157−16164.
(25) CCDC-1865121 contains the supplementary crystallographic data for this paper. These data can be obtained free of charge from The Cambridge Crystallographic Data Centre via www.ccdc.cam.ac.uk/data_request/cif.
(26) Fernández, R.; Melchart, M.; Habtemariam, A.; Parsons, S.; Sadler, P. J. Use of Chelating Ligands to Tune the Reactive Site of Half-Sandwich Ruthenium(II)−Arene Anticancer Complexes. *Chem.—Eur. J.* **2004**, *10*, 5173−5179.
(27) Palmucci, J.; Marchetti, F.; Pettinari, R.; Pettinari, C.; Scopelliti, R.; Riedel, T.; Therrien, B.; Galindo, A.; Dyson, P. J. Synthesis, Structure, and Anticancer Activity of Arene-Ruthenium(II) Complexes with Acylpyrazolones Bearing Aliphatic Groups in the Acyl Moiety. *Inorg. Chem.* **2016**, *55*, 11770−11781.
(28) For examples with the RhCl(COD) fragment, see: (a) Reference 21; (b) Benhamou, L.; Vujkovic, N.; César, V.; Gornitzka, H.; Lugan, N.; Lavigne, G. Facile Derivatization of a "Chemo-active" NHC Incorporating an Enolate Backbone and Relevant Tuning of Its Electronic Properties. *Organometallics* **2010**, *29*, 2616−2630. (c) César, V.; Lugan, N.; Lavigne, G. Electronic Tuning of a Carbene Center via Remote Chemical Induction, and Relevant Effects in Catalysis. *Chem.—Eur. J.* **2010**, *16*, 11432−11442.
(29) Lazreg, F.; Cordes, D. B.; Slawin, A. M. Z.; Cazin, C. S. J. Synthesis of Homoleptic and Heteroleptic Bis-N-heterocylic Carbene Group 11 Complexes. *Organometallics* **2015**, *34*, 419−425.
(30) Díez-González, S.; Stevens, E. D.; Scott, N. M.; Petersen, J. L.; Nolan, S. P. Synthesis and Characterization of [Cu(NHC)$_2$]X Complexes: Catalytic and Mechanistic Studies of Hydrosilylation Reactions. *Chem.—Eur. J.* **2007**, *14*, 158−168.
(31) For a leading reference, please see: Winter, A.; Schubert, U. S. Synthesis and characterization of metallo-supramolecular polymers. *Chem. Soc. Rev.* **2016**, *45*, 5311−5357.
(32) The 1e-oxidation of acac moiety is a well-known process and was documented repeatedly in literature. For relevant examples, see: (a) Jiao, J.; Zhang, Y.; Devery, J. J.; Xu, L.; Deng, J.; Flowers, R. A. Mechanistic Studies of Ce(IV)-Mediated Oxidation of β-Dicarbonyls: Solvent-Dependent Behavior of Radical Cation Intermediates. *J. Org. Chem.* **2007**, *72*, 5486−5492. (b) Song, J.; Zhang, H.; Chen, X.; Li, X.; Xu, D. Oxidative Coupling of 1,3-Dicarbonyl Compounds by Cerium(IV) Ammonium Nitrate. *Synth. Commun.* **2010**, *40*, 1847−1855.
(33) (a) Grineva, A. A.; Valyaev, D. A.; César, V.; Filippov, O. A.; Khrustalev, V. N.; Nefedov, S. E.; Lugan, N. Oxidative Coupling of Anionic Abnormal N-Heterocyclic Carbenes: Efficient Access to Janus-Type 4,4′-Bis(2H -imidazol-2-ylidene)s. *Angew. Chem., Int. Ed.* **2018**, *57*, 7986−7991. (b) Prades, A.; Peris, E.; Alcarazo, M. Pyracenebis(imidazolylidene): A New Janus-Type Biscarbene and Its Coordination to Rhodium and Iridium. *Organometallics* **2012**, *31*, 4623−4626. (c) Wolf, S.; Plenio, H. Synthesis of (NHC)Rh(cod)Cl and (NHC)RhCl(CO)2 complexes - Translation of the Rh- into the Ir-scale for the electronic properties of NHC ligands. *J. Organomet. Chem.* **2009**, *694*, 1487−1492.
(34) Connelly, N. G.; Geiger, W. E. Chemical Redox Agents for Organometallic Chemistry. *Chem. Rev.* **1996**, *96*, 877−910.
(35) Fulmer, G. R.; Miller, A. J. M.; Sherden, N. H.; Gottlieb, H. E.; Nudelman, A.; Stoltz, B. M.; Bercaw, J. E.; Goldberg, K. I. NMR Chemical Shifts of Trace Impurities: Common Laboratory Solvents, Organics, and Gases in Deuterated Solvents Relevant to the Organometallic Chemist. *Organometallics* **2010**, *29*, 2176−2179.
(36) Giordiano, G.; Crabtree, R. H. Di-μ-Chloro-Bis(η^4-1,5-Cyclooctadiene)-DiRhodium(I). *Inorg. Synth.* **1990**, *28*, 88 DOI: 10.1002/9780470132593.ch22.
(37) Bennett, M. A.; Huang, T.-N.; Matheson, T. W.; Smith, A. K. (η^6-Hexamethylbenzene)Rutheniuml Complexes. *Inorg. Synth.* **1982**, *21*, 74 DOI: 10.1002/9780470132524.ch16.
(38) Jensen, S. B.; Rodger, S. J.; Spicer, M. D. Facile preparation of η^6-p-cymene ruthenium diphosphine complexes. Crystal structure of [(η^6-p-cymene)Ru(dppf)Cl]PF$_6$. *J. Organomet. Chem.* **1998**, *556*, 151−158.
(39) Santoro, O.; Collado, A.; Slawin, A. M. Z.; Nolan, S. P.; Cazin, C. S. J. A general synthetic route to [Cu(X)(NHC)] (NHC = N-heterocyclic carbene, X = Cl, Br, I) complexes. *Chem. Commun.* **2013**, *49*, 10483−10485.
(40) Collado, A.; Gómez-Suárez, A.; Martin, A. R.; Slawin, A. M. Z.; Nolan, S. P. Straightforward synthesis of [Au(NHC)X] (NHC = N-heterocyclic carbene, X = Cl, Br, I) complexes. *Chem. Commun.* **2013**, *49*, 5541−5543.
(41) Farrugia, L. J. WinGXsuite for small-molecule single-crystal crystallography. *J. Appl. Crystallogr.* **1999**, *32*, 837−838.
(42) Altomare, A.; Cascarano, G.; Giacovazzo, C.; Guagliardi, A.; Burla, M. C.; Polidori, G.; Camalli, M. SIRPOW.92 - a program for automatic solution of crystal structures by direct methods optimized for powder data. *J. Appl. Crystallogr.* **1994**, *27*, 435−436.
(43) Sheldrick, G. M. *SHELXL-2014/7: Program for the Solution of Crystal Structures*; University of Göttingen: Göttingen, Germany, 2014.

DOI: 10.1021/acsomega.8b02268
ACS Omega 2018, 3, 15582−15591